

NUMERICAL ANALYSIS TO INVESTIGATE THE FIBER SIZE EFFECTS ON COMPOSITE STRENGTH

N.M. Awlad Hossain

Department of Engineering and Design, Eastern Washington University, Cheney, USA

ABSTRACT

Currently many metallic structures are replaced with advanced composites to minimize the structural weight. The primary focus of this research was to examine the effects of fiber geometry to improve the strength of composites, and to pursue the possible advantages of using nanofibers instead of conventional fibers. Three different RVE models were analyzed where the fiber volume fraction kept constant through using reduced fiber diameter. Therefore, the surface area of fiber was increased gradually in each RVE model. The effects of fiber geometry were studied by comparing axial and shear stresses. As the cross sectional area of fiber remained the same in all RVE models, the axial stress of fiber was found relatively unchanged. The surface area of fiber was found important in shear stress distribution. The shear stress of fiber was found to be reduced significantly with increasing its surface area. An RVE model with the highest surface area of fiber was found to offer the lowest shear stress compared to the other RVE models. Therefore, if the composite strength depends on surface area of fiber, then a composite consisting of nanofibers will be stronger than a conventional composite prepared with same volume fraction, or conversely will be lighter at the same strength.

Keywords: Composite, Fiber Volume Fraction, Representative Volume Element.

1. INTRODUCTION

Structural weight reduction with improved strength is one of the targeted outcomes of composite materials. Currently, many metallic structures are replaced with advanced lightweight composites. The primary focus of this research was to examine the effects of fiber geometry to improve the strength of composite materials. The proposed research investigated the possible advantages of using nanofibers instead of conventional fibers. Mathematically, it can be shown that the nanofiber composite contains significantly more surface area over the conventional composite at no cost of volume fraction. The increased surface area can help to compensate for the imperfect bonding between the fiber-matrix interphase. Therefore, composite materials consisting of nanofibers are expected to offer higher strength than a conventional composite prepared with the same volume fraction.

Composite materials (or composites for short) are engineered materials made from two or more constituent materials with significantly different physical or chemical properties, and remain separate and distinct on a microscopic level within the finished structure. The two constituent materials are matrix and fiber (or reinforcement). The matrix material surrounds and supports the fiber materials by maintaining their relative positions. The fibers impart their special mechanical and physical properties to enhance the matrix properties. A synergism produces material properties unavailable from

the individual constituent materials, while the wide variety of matrix and fiber materials allows the designer of the product or structure to choose an optimum combination. Figure 1(a) represents a simplified concept of composite material with fiber and matrix constituents. Figure 1(b) depicts the Representative Volume Element (RVE) – the smallest cell, as shown by dotted line, to describe the individual composite constituents. The RVE is then divided into four subcells, as shown in Figure 1(c), all of rectangular geometry.

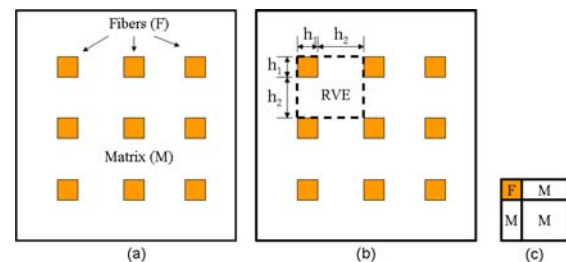


Fig 1. Simplified concept of composite materials and the Representative Volume Element (RVE).

In a series of papers documented by Dr. Jacob Aboudi [1, 2], the overall behavior of composite materials was explored through micromechanical analysis. The analysis was performed using an RVE approach to predict the elastic, thermoelastic,

viscoelastic and viscoplastic responses of composites. The composite material was assumed homogeneously anisotropic continuum without considering the interaction effects between fibers and matrix. Goh et al. [3] developed an analytical solution describing the average fiber stress (σ_f), where the fiber was surrounded by an elastic matrix. The model proposed in [3] consists of a differential equation whose solution provided the distribution of fiber stress (σ_f) and shear stress between fiber and matrix (τ) as a function of length. Expressions for (σ_f) and (τ) were derived without considering the effect of fiber geometry and fiber-fiber interaction. According to the micromechanics theory, an increase in strength cannot be obtained from scaling fiber size while maintaining the same fiber volume fraction. Assuming a unit depth, volume fraction (V_f) of fiber for the RVE model is defined as follows

$$V_f = \frac{h_1^2}{(h_1 + h_2)^2} \quad (1)$$

It can be seen that if the volume fraction is maintained while scaling h_1 down, this will directly affect the value of h_2 . Consequently, the ratio h_1/h_2 in the micromechanics equation will remain the same, and therefore not affect the strength at all. In conclusion, higher strength to weight ratios cannot be obtained from scaling fiber size down at constant volume fraction.

One of the focal points of the proposed research was to determine the strength of composites by creating a more effective RVE model that incorporated the effects of fiber geometry. It has been suggested through other studies that the surface area (A_s) of fibers plays an important role in strength of the composites. An advantage of using nanofibers is to increase the surface area, which can help to compensate for imperfect bonding. Figure 2 illustrates the concept of maintaining the same fiber cross-sectional area while increasing fiber surface area.

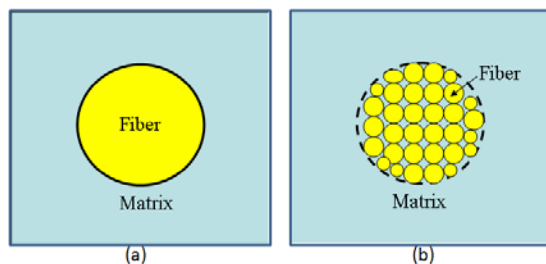


Fig 2. (a) Illustration of RVE of conventional composite with single unidirectional fiber. (b) Illustration of RVE of modified nanocomposite with many unidirectional fibers.

Mathematically it can be proved that the surface area of fiber in nanofiber composite will be higher than that of conventional composite by a factor of \sqrt{N} , where N represents the total number of nano fibers. Therefore, if the composite strength depends on fiber surface area, then a composite consisting of nanofibers will be stronger than a conventional composite prepared with

same volume fraction. However, this strength advantage is not apparent in Aboudi's micromechanics theory. The primary purpose of this research was to examine the effects of fiber geometry, and pursuing the possible advantages of utilizing nanofibers within composite materials.

2. ANALYSIS

A. Numerical Models

Numerical models of conventional and nanofiber composites were developed using nonlinear finite element code ABAQUS and ANSYS. First, three different RVE models were developed as shown in Figure 3. For simplicity in the following sections, these numerical models are called RVE-1, RVE-2, and RVE-3. Note that all dimensions are in micrometer (μm).

RVE-1, as shown in Figure 3(a), represents a conventional composite with one complete fiber connected with matrix. RVE-2, as shown in Figure 3(b) represents a nanofiber composite, with two nano fibers (one complete + four quarters) connected with matrix. Similarly, RVE-3, as shown in Figure 3(c), also represents a nanofiber composite with four nano fibers (one complete + 4 halves + 4 quarters). In RVE-2 and RVE-3, the fiber size was scaled down from radial dimension 5 micron to 3.5 micron and 2.5 micron, respectively. All RVE models have the same volume fraction of fiber (20%). The surface area of fiber in RVE-2 and RVE-3 was increased by 40% and 100%, respectively compared to the RVE-1. For analysis simplicity and to minimize the computational time, quarter symmetric models of the conventional and nanofiber composites, as shown in Figure 4, were used.

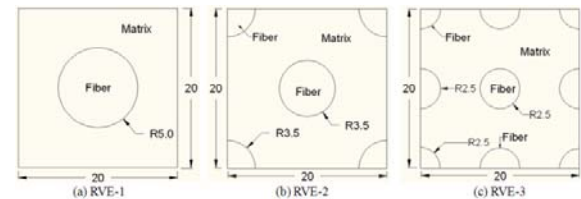


Fig 3. Illustration of different RVE model with increased fiber surface area while keeping the same fiber volume fraction.

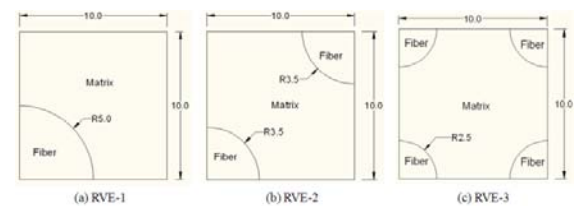


Fig 4. Quarter symmetric models of conventional and nanofiber composites used in the numerical analysis.

B. Boundary Conditions and Loading

Numerical analyses were performed with the following boundary conditions and loading. For better understanding, a 3D view of the quarter symmetric conventional composite model is shown in Figure 5. The

entire back surface ($z = 0$), which contains both fiber and matrix nodes, was constrained in its normal direction.

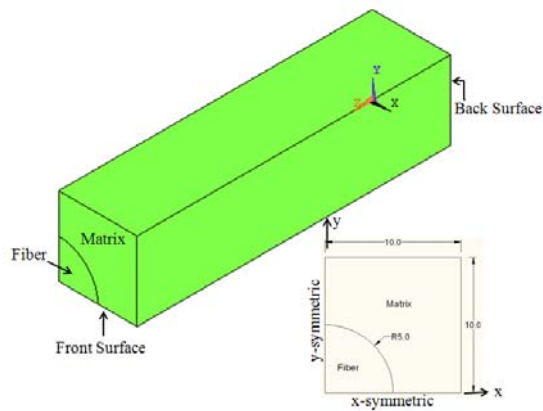


Fig 5. 3D view of the conventional composite model.

Symmetric boundary conditions were applied at the left and bottom edges. In addition, to constrain the rotational motion, two adjacent sides ($x = 10$, and $y = 10$) were also constrained to their normal directions. Also, one node point on the back surface was pinned to prevent translation in the global x - and y - directions. Boundary displacement loading was assigned only to the matrix nodes of the front surface.

The fiber surface was connected by ties to all correlated matrix surface. The numerical model did not consider any interphase zone. The other quarter symmetric models, as shown in Figure 4, were also analyzed using the same boundary conditions and loading as discussed above.

C. Material Properties

The materials properties are simply elastic and include Young's modulus and Poisson's ratio. Standard mechanical properties of E-glass and Epoxy were used to mimic the fiber and matrix, respectively.

3. RESULTS AND DISCUSSION

The following results were obtained when the entire back surface was constrained to its normal direction, and the boundary displacement was applied to matrix at the front surface. All three quarter symmetric models, as shown in Figure 4, were analyzed. For each case, axial and shear stress distribution of the fiber was studied. As the matrix region of nanofiber composite models has different geometry compared to the conventional composite, boundary displacement assigned to the nanofiber composites was tuned until they offered the same reaction force (at the back surface) found for the conventional composite model.

First, we compared the stress distribution of the RVE-1 and RVE-2. The axial stress distribution along a nodal path coincident with the fiber axis ($x = 0$ and $y = 0$) is shown in Figure 6. The cross sectional area of fiber remains the same between the conventional and nanofiber composite models. Therefore, the axial stress distribution was found to be fairly unchanged. The axial stress was found higher near the fixed end and gradually

decreased near the free end where load was applied. The numerical results match with expected outcomes.

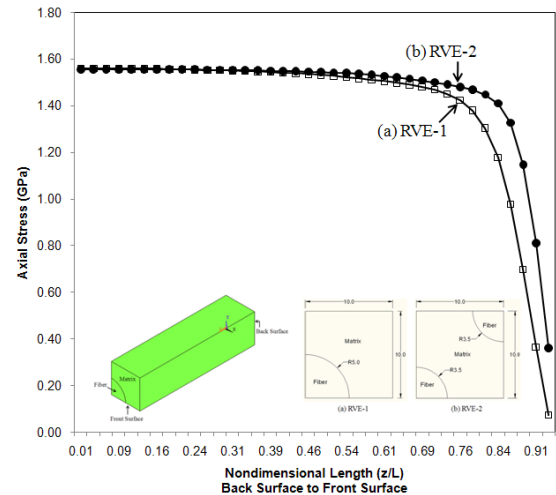


Fig 6. Axial stress (z -direction) distribution along the fiber axis between conventional and nanofiber composite models.

The shear stress distribution along a nodal path (at angular orientation $\theta = 90$ degree – as named 12 o'clock section) on the topmost fiber layer is shown in Figure 7. The surface area of fiber was increased by 40% in the RVE-2 compared to the RVE-1. Therefore, the shear stress distribution in the RVE-2, representing a nanofiber composite, was found significantly reduced. A closer observation of the shear stress distribution, up to nondimensional length (z/L) equal to 0.5, is shown in Figure 8. Shear stress in the RVE-2 was found to be reduced by approximately 50% compared to the RVE-1. Shear stress was also found to be smaller near the fixed end and increased exponentially towards the free end. The numerical results also match with expected outcomes.

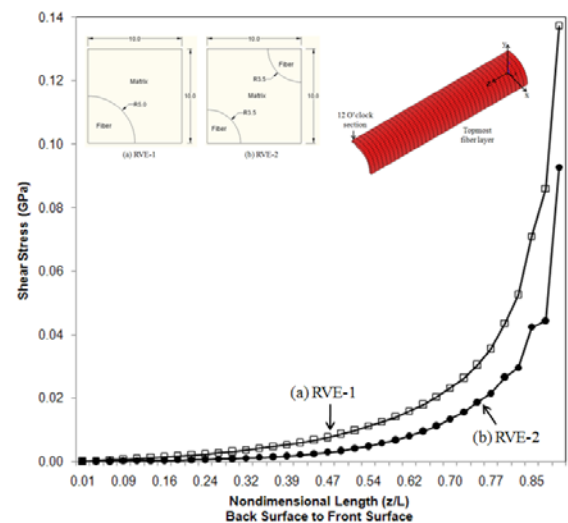


Fig 7. Shear stress distribution along a nodal path (at 12 o'clock section) on the topmost fiber layer between the conventional and nanofiber composite models.

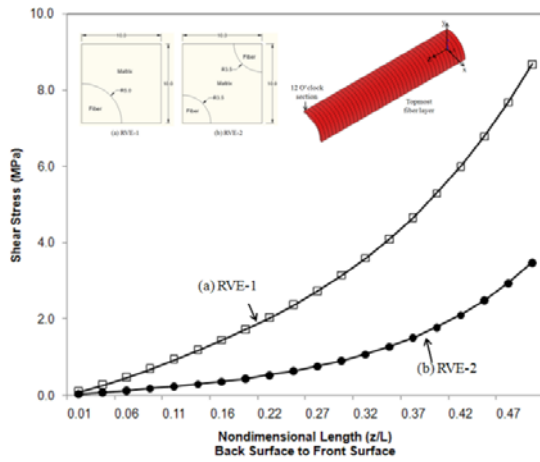


Fig 8. Shear stress (yz -direction) distribution along a nodal path (at 12 o'clock section) on the topmost fiber layer between the conventional and nanofiber composite. A closer view, $z/L = 0$ to 0.5 , is shown.

The axial stress distribution along the fiber axis of all three different RVE models is shown in Figure 9. As the fiber cross sectional area is the same in each RVE model, the axial stress was found almost unchanged up to the nondimensional length (z/L) equal to 0.75 . Some discrepancies were observed near the free end where boundary displacement was applied.

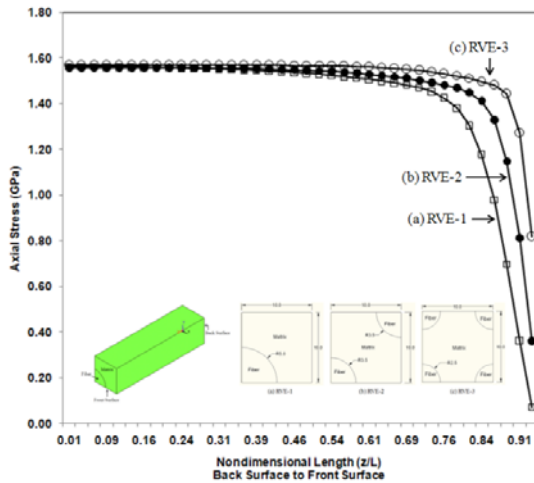


Fig 9. Axial stress (z -direction) distribution along a nodal path coincident to the fiber axis between the conventional and two other nanofiber composites.

On the other hand, the shear stress distribution of the topmost fiber layer of all three different RVE models is shown in Figure 10. The shear stress in the RVE-2 and RVE-3, representing nanofiber composites, was found to be reduced more with increasing the fiber surface area. The surface area of fiber in the RVE-3 is 60% more compared to the RVE-2. Subsequently, the shear stress in the RVE-3 was also found much smaller compared to the RVE-2.

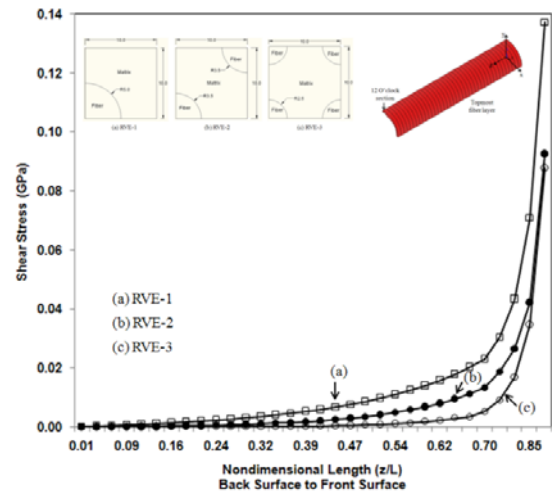


Fig 10. Shear stress distribution along a nodal path (at 12 o'clock section) on the topmost fiber layer between the conventional and two other nanofiber composite models.

For closer observation, the shear stress distribution of RVE-3, up to nondimensional length (z/L) equal to 0.50 , is plotted separately with RVE-1 and RVE-2. These results are shown in Figures 11 and 12, respectively. The surface area of fiber in RVE-3 is increased by 100% compared to the RVE-1, and by 60% compared to RVE-2. Shear stress of the fiber, as shown in Figures 11 and 12, is expected to decrease more with further increment of its surface area.

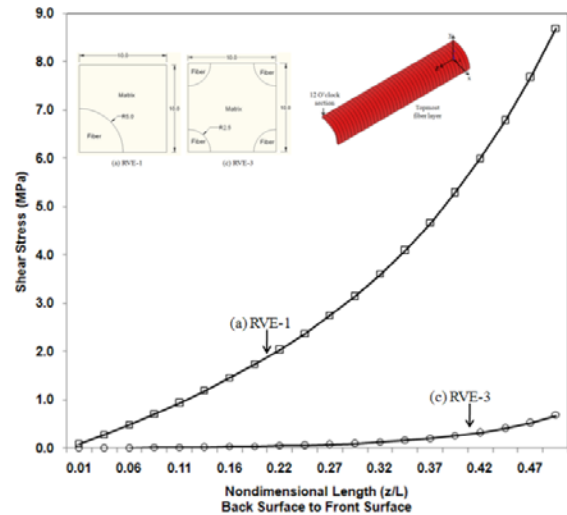


Fig 11. Shear stress (yz -direction) distribution along a nodal path (at 12 o'clock section) on the topmost fiber layer between the conventional and nanofiber composite, RVE-3.

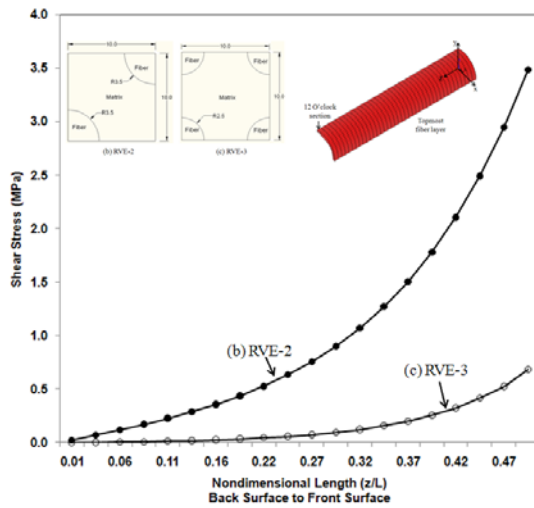


Fig 12. Shear stress (yz-direction) distribution along a nodal path (at 12 o'clock section) on the topmost fiber layer between two nanofiber composites RVE-2 and RVE-3.

Numerical simulation of the RVE models was then repeated with changing the boundary condition as follows. Instead of constraining the entire back surface, only the fiber nodes at the back surface were constrained to their normal z-direction. Therefore, matrix nodes at the back surface were released to translate along the global z-direction. Boundary displacement was assigned to the matrix nodes at the front surface, as used before.

The shear stress distribution of the three different RVE models is shown in Figure 13. Due to change in boundary condition, the shear stress distribution pattern observed in Figure 13 is significantly different from Figure 10. Shear stress was found to be smaller near the mid section and increased exponentially towards the fixed and free ends. However, as the surface area of fiber was increased in the RVE-2 & RVE-3, the shear stress in RVE-2 & RVE-3 was found significantly reduced compared to the RVE-1.

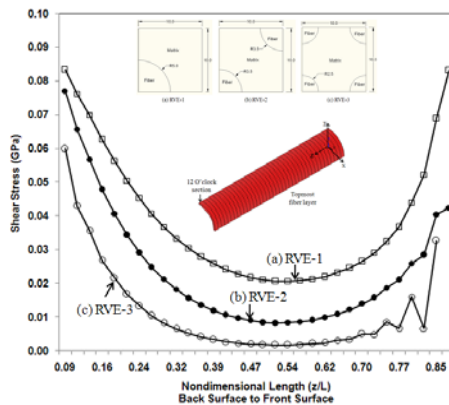


Fig 13. Shear stress (yz-direction) distribution along a nodal path (on 12 o'clock section) on the topmost fiber layer between conventional and two nanofiber composite models.

4. CONCLUSION

In this paper, the effect of fiber geometry on composite strength was studied by numerical simulations. Three different RVE models were used where the surface area of fiber was increased gradually, keeping the fiber volume fraction constant. As the cross sectional area of fiber remained the same in all RVE models, the axial stress of fiber was found almost unchanged. The shear stress of fiber was found to be reduced significantly with increasing the surface area of fiber. An RVE model with the highest surface area of fiber was found to offer the lowest shear stress compared to the other RVE models. Numerical simulations were repeated with changing the boundary conditions. In all cases, an RVE model with increased surface area of fiber was found to offer reduced shear stress. Therefore, on the basis of shear stress developed in the fiber region, a composite consisting of nanofibers will be stronger than a conventional composite prepared with same fiber volume fraction, or conversely will be lighter at the same strength.

5. REFERENCES

1. Aboudi, J., "Micromechanical Analysis of Composites by the Method of Cells," ASME, 1989.
2. Aboudi, J., "Micromechanics Prediction of Fatigue Failure of Composite Materials," Journal of Reinforced Plastic Composites, 1989.
3. Goh, K.L., Aspden, R.M., and Hukins, D.W.L., "Shear Lag Models for Stress Transfer from an Elastic Matrix to a Fiber in a Composite Materials," Int. J. Materials and Structural Integrity, Vol. 1, Nos. 1/2/3, 2007.

6. NOMENCLATURE

| Symbol | Meaning | Unit |
|------------|-------------------------------|-------------------|
| RVE | Representative volume element | |
| σ_f | Fiber axial stress | (Pa) |
| τ | Shear stress | (Pa) |
| V_f | Fiber volume fraction | |
| h_1 | Dimension of fiber | (μm) |
| h_2 | Dimension of matrix | (μm) |
| N | Number of nanofibers | |

7. MAILING ADDRESS

N.M. Awlad Hossain
 Assistant Professor
 Department of Engineering and Design
 Eastern Washington University
 Cheney, WA-99004, USA